Brief Communications

The σ-1 Receptor Interacts Directly with GluN1 But Not GluN2A in the GluN1/GluN2A NMDA Receptor

Dilshan Balasuriya, Andrew P. Stewart, and J. Michael Edwardson
Department of Pharmacology, University of Cambridge, Cambridge CB2 1PD, United Kingdom

The σ-1 receptor (Sig1R) is widely expressed in the CNS, where it has a neuroprotective role in ischemia and stroke and an involvement in schizophrenia. The Sig1R interacts functionally with a variety of ion channels, including the NMDA receptor (NMDAR). Here, we used atomic force microscopy (AFM) imaging to investigate the interaction between the Sig1R and the NMDAR. The Sig1R bound directly to GluN1/GluN2A NMDAR heterotetramers. Furthermore, the mean angle between pairs of bound Sig1Rs was 72°. This result suggested that the Sig1R interacts with either GluN1 or GluN2A, but not both, and supports our recent demonstration that the NMDAR subunits adopt an adjacent (i.e., 1/1/2/2) arrangement. The Sig1R could be coisolated with GluN1 but not with GluN2A, indicating that GluN1 is its specific target within the NMDAR. Consistent with this conclusion, AFM imaging of coisolated Sig1R and GluN1 revealed GluN1 dimers decorated with Sig1Rs. *In situ* proximity ligation assays demonstrated that the Sig1R interacts with GluN1 (but not with GluN2A) within intact cells and also that its C terminus is extracellular. We conclude that the Sig1R binds to the GluN1/GluN2A NMDAR specifically via the GluN1 subunit. This interaction likely accounts for at least some of the modulatory effects of Sig1R ligands on the NMDAR.

Introduction

The σ-1 receptor (Sig1R) is widely distributed throughout the CNS, where it participates in processes such as neurotransmitter release, and learning and memory (Maurice and Su, 2009). It has also been shown to contribute to neuroprotection in cerebral ischemia and stroke (Lysko et al., 1992) and has been genetically linked to schizophrenia (Ishiguro et al., 1998). The Sig1R can bind many ligands including antipsychotic drugs (e.g., haloperidol), psychotomimetics (e.g., pentazocine), and steroids (e.g., progesterone; Su et al., 2010).

Many effects mediated through the Sig1R are likely based on its ability to modulate a variety of voltage- and ligand-gated ion channels (Su et al., 2010). Previous studies, based on coimmunoprecipitation, have suggested that the actions of Sig1Rs on ion channels such as Kv1.4 (Aydar et al., 2002), the human ether-á-go-go-related gene (hERG) potassium channel (Crottès et al., 2011), and the L-type Ca^{2+} ion channel (Tchedre et al., 2008) are via a direct interaction. Recently, using atomic force microscopy (AFM) imaging, we have shown that the Sig1R interacts with the trimeric acid-sensing ion channel 1a with threefold symmetry (Carnally et al., 2010) and with the Nav1.5 voltage-gated Na^+ channel with fourfold symmetry (Balasuriya et al., 2012).

The Sig1R is known to affect the function of the NMDA receptor (NMDAR). NMDARs are found in nearly all CNS neurons and play a critical role in synaptic plasticity and neuronal development (Traynelis et al., 2010); they are also key players in glutamatergic excitotoxicity (Waxman and Lynch, 2005). Sig1R ligands have been shown to prevent neuronal cell death mediated through glutamate excitotoxicity in the CNS, both *in vitro* (Lysko and Feuerstein, 1990) and *in vivo* (Lysko et al., 1992). However, whether the ligands are acting through the Sig1R (e.g., Hayashi et al., 1995) or through a direct effect on the NMDAR (Kume et al., 2002) has been controversial. In the present study, we set out to elucidate the nature of the interaction between the Sig1R and the NMDAR. We show, using protein coisolation and AFM imaging, that the Sig1R binds directly to the GluN1/GluN2A NMDAR specifically via GluN1. We also use *in situ* proximity ligation to demonstrate that this interaction occurs within cells.

Materials and Methods

Cell culture. The tsA 201 and NG108-15 cells were grown in DMEM supplemented with 10% (v/v) fetal bovine serum, 100 μg/ml streptomycin, and 100 U/ml penicillin in an atmosphere of 5% CO_2/air.

Constructs. The following constructs were used: human Sig1R, with either a FLAG/His_6 epitope tag or a V5/His_6 tag at the C terminus; wild-type rat GluN1–1a; GluN1 with a hemagglutinin (HA)/His_8 tag between residues 416 and 417 in the agonist-binding domain (ABD); GluN1 with an HA/His_8 tag between residues 842 and 843, which is 10 residues downstream of the transmembrane domain (TMD); GluN2A with a FLAG/His_8 epitope tag between residues 851 and 852, which is 15 residues downstream of the TMD; and GluN2A with an HA/His_8 tag between residues 425 and 426 in the ABD. All constructs were in the vector pcDNA3.1. Neither the His_6 tag on the Sig1R nor the His_8 tags on GluN1 and GluN2A were used in the experiments described here; they are, therefore, omitted from subsequent references to the constructs.

Received Aug. 7, 2013; revised Sept. 30, 2013; accepted Oct. 7, 2013.

Author contributions: J.M.E. designed research; D.B. and A.P.S. performed research; D.B. and A.P.S. analyzed data; D.B. and J.M.E. wrote the paper.

This work was supported by the Wellcome Trust (J.M.E.). D.B. holds a David James Bursary from the Department of Pharmacology. A.P.S. was supported by the Jean Shanks Foundation and the James Baird Fund.

The authors declare no competing financial interests.

This article is freely available online through the *J Neurosci* Author Open Choice option.

Correspondence should be addressed to J. Michael Edwardson at the above address. E-mail: jme1000@cam.ac.uk.

DOI:10.1523/JNEUROSCI.3360-13.2013

Isolation of epitope-tagged proteins. The tsA 201 and NG108-15 cells were transfected with DNA using calcium phosphate precipitation. In all cases, 250 μg of DNA was used to transfect 5 × 162 cm^2 flasks. For cotransfections, equal amounts of DNA were used for each construct. After transfection, cells were incubated for 48 h at 37°C to allow protein expression. The NMDAR antagonists, 2-amino-5-phosphonovaleric acid (2 μM), 5,7-dichlorokynurenic acid (1 μM), and MK801 (2 μM), were added to the medium to prevent cell toxicity.

Transfected cells were solubilized in 1% (v/v) Triton X-100 for 1 h at 4°C before centrifugation at 62,000 × *g* to remove all insoluble material. To capture Sig1R-FLAG or GluN2A-FLAG, the solubilized extract was incubated with anti-FLAG–agarose beads (Sigma-Aldrich) for 3 h. The beads were washed extensively, and bound protein was eluted with triple-FLAG peptide (100 μg/ml). The eluted samples were analyzed by SDS-PAGE, followed by immunoblotting using the following antibodies, as appropriate: mouse monoclonal anti-FLAG (clone M2; Sigma-Aldrich), mouse monoclonal anti-V5 (Invitrogen), mouse monoclonal anti-GluN1 (ab134308, raised against amino acids 42–361 of GluN1; Abcam), and rabbit monoclonal anti-GluN2A (clone A12W, raised against residues 1265–1464 of mouse GluN2A; Millipore).

AFM imaging of isolated proteins. Isolated proteins were applied to freshly cleaved mica disks, washed, and dried under a stream of nitrogen. AFM imaging was performed exactly as described previously (Balasuriya et al., 2013).

For particles within complexes, particle heights and diameters were measured manually by the Nanoscope software and used to calculate the molecular volume of each particle using the following equation:

$$V_m = (\pi h/6)(3r^2 + h^2), \quad (1)$$

where h is the particle height and r is the radius (Schneider et al., 1998). This equation assumes that the adsorbed particles adopt the form of a spherical cap. Molecular volume based on molecular mass was calculated using the following equation:

$$V_c = (M_0/N_0)(V_1 + dV_2), \quad (2)$$

where M_0 is the molecular mass; N_0 is Avogadro's number; V_1 and V_2 are the partial specific volumes of particle (0.74 cm^3/g) and water (1 cm^3/g), respectively; and d is the extent of protein hydration (taken as 0.4 g water/g protein).

Selection of binding events. To be accepted, bound Sig1Rs needed to have a molecular volume between 30 and 120 nm^3, and Sig1R-decorated NMDAR particles needed to have volumes in the range of 800–2000 nm^3. The height of the lowest point between the two particles needed to be >0.3 nm for the peripheral particle to be considered bound. Any particle with a length greater than twice its width was rejected. To be considered a double-binding event, all particles and both binding events needed to meet the above criteria.

Molecular volumes for undecorated NMDARs were determined using the Scanning Probe Image Processor version 5 (Image Metrology). The volume range 800–2000 nm^3 was used to identify NMDAR tetramers.

Statistical analysis. Histograms were drawn with bin widths chosen according to Scott's equation:

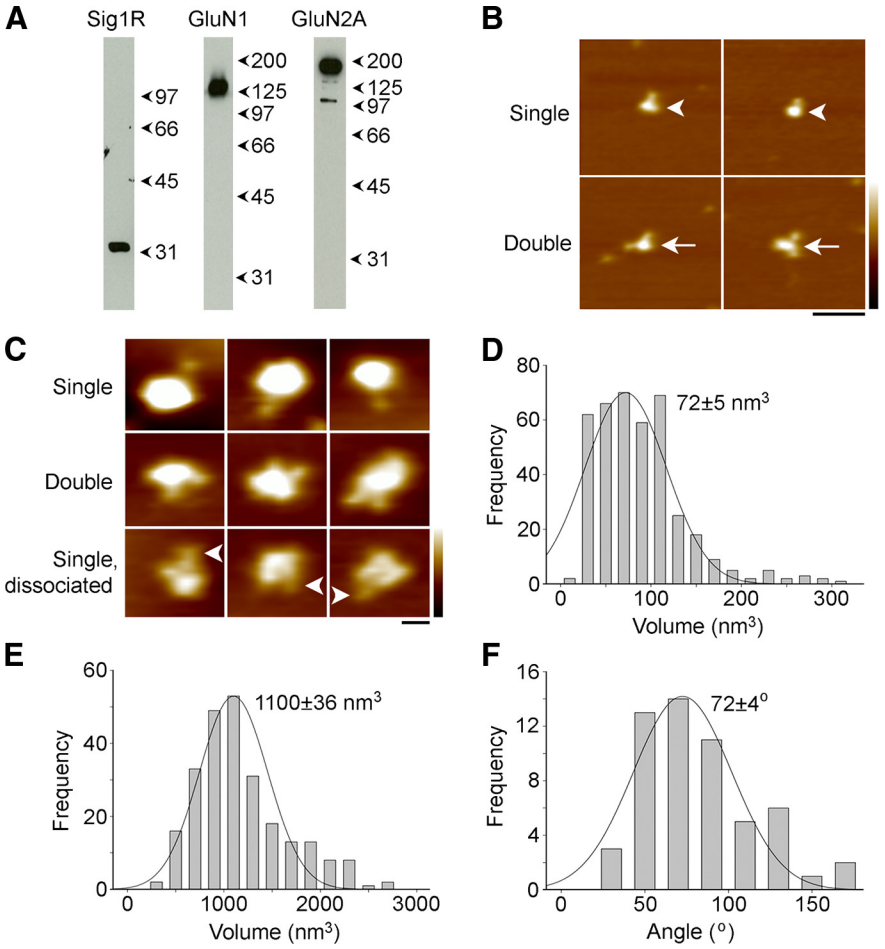

Figure 1. Decoration of GluN1/GluN2A NMDA receptors by Sig1Rs. ***A***, The protein isolated from tsA 201 cells expressing Sig1R-V5, wild-type GluN1, and GluN2A-FLAG by anti-FLAG immunoaffinity chromatography was analyzed by immunoblotting using anti-V5 (left), anti-GluN1 (middle), or anti-GluN2A (right) monoclonal antibodies. Molecular masses are in kilodaltons. ***B***, Low-magnification AFM images of GluN1/GluN2A NMDARs coexpressed with Sig1Rs. Arrowheads (top) and arrows (bottom) indicate singly and doubly decorated NMDARs, respectively. Scale bar, 50 nm; color-height scale, 0–4 nm. ***C***, Gallery of zoomed AFM images showing singly (top) and doubly (middle) decorated receptors and partially dissociated NMDA receptors with single Sig1Rs (arrowheads) bound to the smaller of the two subunits (bottom). Scale bar, 20 nm; color-height scale, 0–3 nm. ***D***, Frequency distribution of molecular volumes of all bound peripheral particles (Sig1Rs). The curve indicates the fitted Gaussian function. The peak of the distribution is indicated. ***E***, Frequency distribution of molecular volumes of the Sig1R-decorated central particles. ***F***, Frequency distribution of angles between pairs of Sig1Rs bound to NMDARs.

$$\text{Bin width} = 3.5\sigma/n^{1/3}, \quad (3)$$

where σ is an estimate of the SD and n is the sample size (Scott, 1979). Where Gaussian curves were fitted to the data, the number of curves was chosen to maximize the r^2 value while giving significantly different means using Welch's t test for unequal sample sizes and unequal variances (Welch, 1947).

In situ proximity ligation assay. The tsA 201 cells growing on lysine- and collagen-coated glass coverslips were cotransfected with 1.5 μg each of DNA encoding Sig1R-FLAG and GluN1-HA (tagged in the ABD), GluN1-HA (tagged downstream of the TMD), or GluN2A-HA (tagged in the ABD). Cells were incubated for 24 h at 37°C to allow protein expression, and the proximity ligation reaction was performed according to the manufacturer's instructions (Olink Bioscience) and as described previously (Balasuriya et al., 2012). Cells were imaged by confocal laser-scanning microscopy.

Results

GluN1 and GluN2A bearing a FLAG epitope downstream of its final TMD were expressed in tsA 201 cells along with Sig1R-V5. All three proteins could be coisolated by anti-FLAG immuno-

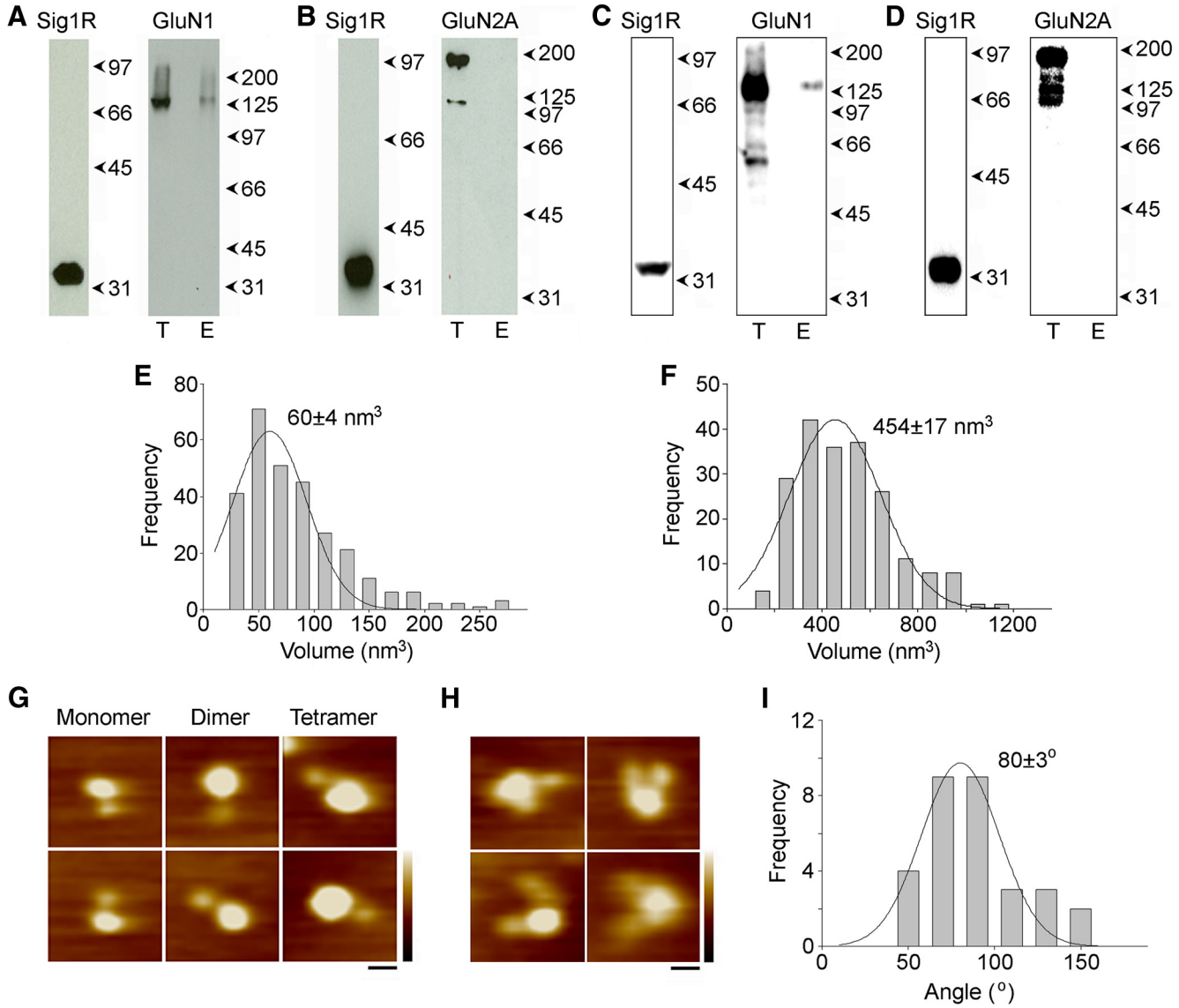

Figure 2. Decoration of GluN1 subunits by Sig1R. ***A***, The protein isolated from tsA 201 cells coexpressing wild-type GluN1 and Sig1R-FLAG by anti-FLAG immunoaffinity chromatography was analyzed by SDS-PAGE, followed by immunoblotting with either anti-FLAG (left) or anti-GluN1 (right) monoclonal antibodies. Both total and eluted samples are shown for GluN1. ***B***, The protein isolated from tsA 201 cells coexpressing wild-type GluN2A and Sig1R-FLAG by anti-FLAG immunoaffinity was analyzed by SDS-PAGE followed by immunoblotting with either anti-FLAG (left) or anti-GluN2A (right) monoclonal antibodies. Both total and eluted samples are shown for GluN2A. ***C***, Immunoblot analysis of protein isolated from NG108-15 cells coexpressing wild-type GluN1 and Sig1R-FLAG. ***D***, Immunoblot analysis of protein isolated from NG108-15 cells coexpressing wild-type GluN2A and Sig1R-FLAG. ***E***, Frequency distribution of volumes of bound peripheral particles (Sig1Rs) for protein isolated from cells coexpressing wild-type GluN1 and Sig1R-FLAG. The curve indicates the fitted Gaussian function. The peak of the distribution is indicated. ***F***, Frequency distribution of volumes of large particles that were decorated by Sig1Rs. ***G***, Zoomed AFM images of single Sig1Rs bound to monomer-, dimer-, and tetramer-sized GluN1 particles. ***H,*** Gallery of zoomed AFM images of GluN1 dimers that were doubly decorated with Sig1Rs. ***I,*** Frequency distribution of angles between pairs of Sig1Rs bound to GluN1 dimers. T, Total; E, eluted. Scale bars, 20 nm; color-height scale, 0–3 nm.

affinity chromatography, as judged by immunoblotting using anti-V5, anti-GluN1, and anti-GluN2A antibodies (Fig. 1*A*). Low-magnification AFM images of the sample are shown in Figure 1*B*. Arrowheads and arrows indicate large particles decorated by one or two smaller particles, respectively. A gallery of singly and doubly decorated large particles is shown in Figure 1*C*. A frequency distribution of the volumes of the smaller particles, calculated using Equation 1, is shown in Figure 1*D*. The distribution had a peak at 72 ± 5 (SEM) nm^3 ($n = 400$), close to the values obtained previously for Sig1Rs alone (Carnally et al., 2010; Balasuriya et al., 2012), and to the expected volume of 63 nm^3 for a Sig1R of molecular mass 33 kDa, calculated using Equation 2. Using this volume distribution, a volume range of 30–120 nm^3 was set for the Sig1R and was used to identify Sig1R-decorated particles. A frequency distribution of volumes of the larger, decorated particles (Fig. 1*E*) had a single peak at 1100 ± 36 nm^3 ($n = 247$), similar to the expected volume of 1140 nm^3 for an intact NMDAR. Hence, the structures shown in Figure 1, *B* and *C*, are complexes between assembled NMDAR tetramers and bound Sig1Rs. The numbers of decorated and undecorated NMDARs (defined as particles in the volume range of 800–2000 nm^3) were counted. Of a total of 1065 receptors, 13.1% (140) were singly decorated and 5.2% (55) were doubly decorated. Corresponding percentages for a control experiment in which GluN1 and GluN2A were expressed without the Sig1R were as follows: 2.5% (23 of 936) singly decorated and 0.6% (6 of 936) doubly decorated. Hence, the majority of the decoration events seen after the triple transfection were specific. A frequency distribution of the

angles between pairs of Sig1Rs bound to NMDARs (Fig. 1*F*) had a single peak at 72 ± 4° ($n = 55$). This result is consistent with a 1/1/2/2 subunit arrangement within the GluN1/GluN2A NMDAR and also indicates that the Sig1R is interacting with either GluN1 or GluN2A, but not both. Figure 1*C* (bottom) shows Sig1Rs (arrowheads) bound to partially dissociated NMDARs via the smaller of the two types of NMDAR subunits, suggesting that the Sig1R might bind to GluN1.

To identify the target subunit of the Sig1R within the NMDAR, Sig1R-FLAG was coexpressed with either wild-type GluN1 or wild-type GluN2A, and the Sig1R was isolated by anti-FLAG immunoaffinity chromatography. After coexpression of the Sig1R with GluN1, immunoblotting demonstrated the coisolation of the two proteins (Fig. 2*A*). In contrast, when Sig1R-FLAG was coexpressed with GluN2A, only the Sig1R and not GluN2A was isolated by anti-FLAG immunoaffinity chromatography (Fig. 2*B*). Hence, the Sig1R binds to GluN1 but not to GluN2A. The specific interaction of the Sig1R with GluN1 was not restricted to tsA 201 cells but was also seen in the neuroblastoma × glioma hybrid cell line NG108-15 (Fig. 2*C*,*D*).

Proteins isolated from tsA 201 cells coexpressing Sig1R and GluN1 were subjected to AFM imaging. A frequency distribution of volumes of bound smaller particles (Fig. 2*E*) had a single peak at 60 ± 4 nm^3 ($n = 287$). A frequency distribution of volumes of the larger, decorated particles had a single peak at 454 ± 17 nm^3 ($n = 193$; Fig. 2*F*), similar to the predicted volume of a GluN1 dimer (456 nm^3). This result suggests that when expressed without GluN2A, GluN1 exists predominantly as a dimer. A gallery of zoomed single-binding events shows examples of Sig1R-decorated monomer-sized (Fig. 2*G*, left), dimer-sized (Fig. 2*G*, middle), and tetramer-sized (Fig. 2*G*, right) particles. To determine the relative proportions of the three assembly states, we set volume ranges of 200–400 nm^3 (monomers), 400–800 nm^3 (dimers), and 800–1300 nm^3 (tetramers) and counted the numbers of decorated particles within these three ranges. We found that 55.3% of all binding events were to dimer-sized particles, whereas 35.7% were to monomer-sized particles and only 9.0% were to tetramer-sized particles. A gallery of doubly decorated GluN1 dimers is shown in Figure 2*H*. No monomer-sized particles were doubly decorated with Sig1Rs, suggesting that each subunit has only one Sig1R-binding site. A frequency distribution of angles between pairs of Sig1Rs bound to GluN1 dimers (Fig.

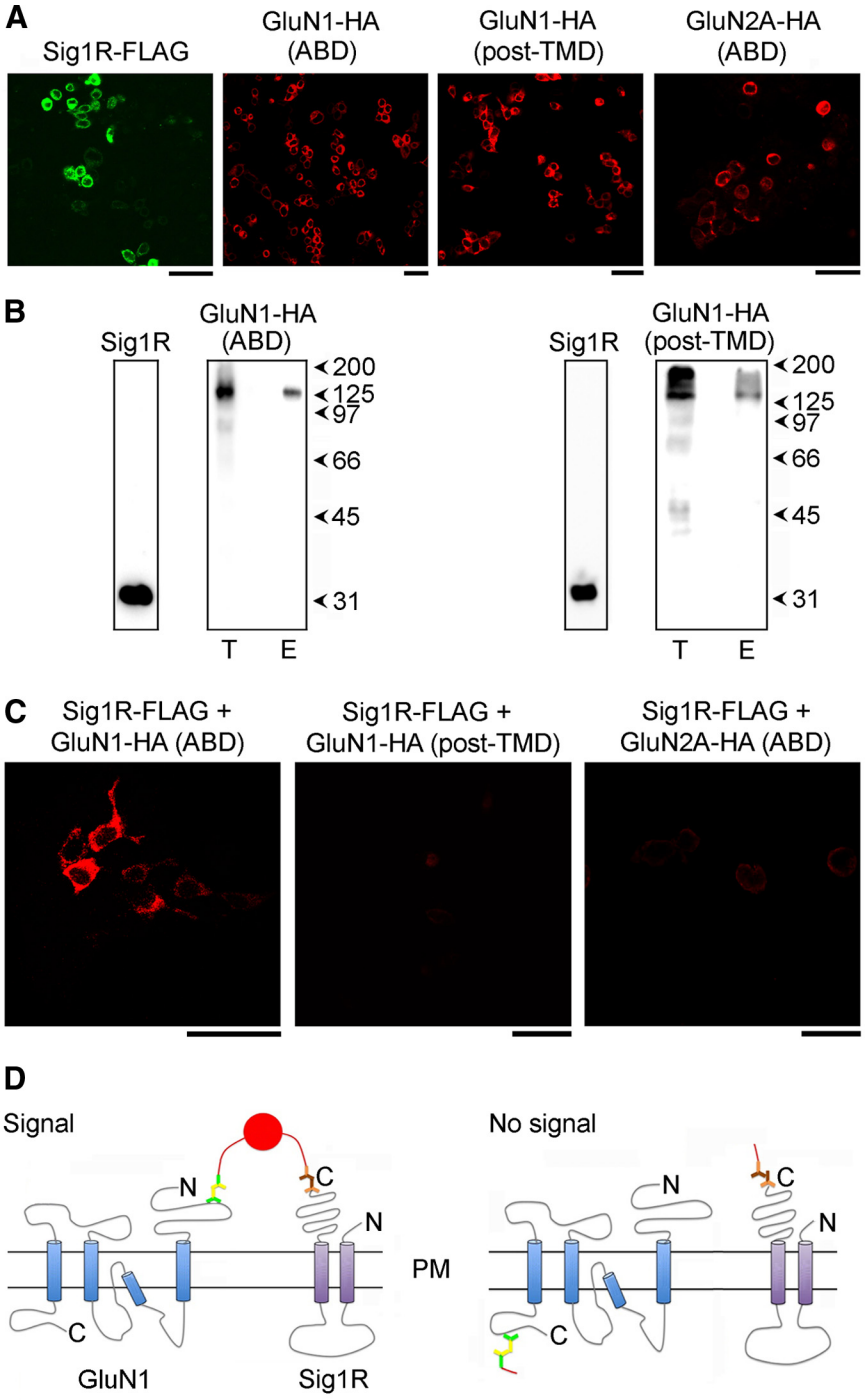

Figure 3. *In situ* proximity ligation assays for interactions of the Sig1R with either GluN1 or GluN2A. ***A***, The tsA 201 cells were transfected individually with DNA encoding Sig1R-FLAG, GluN1-HA (ABD), GluN1-HA (post-TMD), or GluN2A-HA (ABD). Cells were permeabilized and incubated with mouse monoclonal anti-FLAG or rabbit polyclonal anti-HA antibody, as appropriate, followed by fluorescein isothiocyanate-conjugated goat anti-mouse or Cy3-conjugated goat anti-rabbit secondary antibodies. Scale bars, 50 μM. ***B***, The protein isolated from cells expressing Sig1R-FLAG plus either GluN1-HA (ABD; left) or GluN1-HA (post-TMD; right) by anti-FLAG immunoaffinity chromatography was analyzed by immunoblotting, using either anti-FLAG or anti-GluN1 antibodies. Both total (T) and eluted (E) samples are shown for GluN1. ***C***, Cells were cotransfected with DNA encoding Sig1R-FLAG plus GluN1-HA (ABD; left), GluN1-HA (post-TMD; middle), or GluN2A-HA (ABD; right). Cells were fixed, permeabilized, and incubated with primary antibodies (mouse monoclonal anti-FLAG and rabbit polyclonal anti-HA; H6908, Sigma-Aldrich), followed by anti-mouse (+) and anti-rabbit (−) proximity ligation secondary antibodies. The proximity ligation assay was then performed. Scale bars, 50 μM. ***D***, Schematic illustration of the *in situ* proximity ligation assay for Sig1R-FLAG plus GluN1-HA (ABD; left) and Sig1R-FLAG plus GluN1-HA (post-TMD; right). N, N terminus; C, C terminus; PM, plasma membrane.

2*I*) had a single peak at 80 ± 3° ($n = 30$), close to the angle found in complete NMDAR heterotetramers (72°, above).

To determine whether the Sig1R interacts with GluN1 in intact cells, we performed *in situ* proximity ligation assays with Sig1R-FLAG and either GluN1-HA or GluN2A-HA. For GluN1-HA, the tag was either in the ABD (extracellular) or post-TMD (intracellular). The assay (Söderberg et al., 2006) uses two secondary antibodies, each bearing a short DNA strand. When the secondary antibodies are brought into close proximity (<40 nm) by binding to their relevant primary antibodies, the DNA strands hybridize with an additional circle-forming oligodeoxynucleotide. Ligation then creates a complete circularized oligodeoxynucleotide, and rolling circle amplification increases the amount of circular DNA several hundredfold. The DNA is then visualized using a fluorescent probe. The immunofluorescence images in Figure 3*A* show that for all four constructs, the epitope tag was detected by its appropriate antibody. Moreover, both GluN1-HA (ABD) and GluN1-HA (post-TMD) were efficiently coisolated with Sig1R-FLAG (Fig. 3*B*), indicating that the presence of the tag in either position did not interfere with the *in vitro* interaction between the Sig1R and GluN1. The *in situ* proximity ligation assays gave a bright signal with cells coexpressing both Sig1R-FLAG plus GluN1-HA (ABD), but not with cells expressing Sig1R-FLAG plus GluN1-HA (post-TMD) or Sig1R-FLAG plus GluN2A (ABD; Fig. 3*C*). This result demonstrates that the Sig1R interacts with GluN1 (but not with GluN2A) within intact cells; it also indicates that the C terminus of the Sig1R (and, consequently, the N terminus also) must be extracellular. A schematic illustration of the interaction between the Sig1R and GluN1 is shown in Figure 3*D*.

Discussion

We show here that the Sig1R interacts with the GluN1/GluN2A NMDAR directly and specifically via GluN1, a subunit that is believed to be present in all NMDARs. This physical interaction is consistent with a number of reports that Sig1R ligands can modulate the activity of NMDARs in neurons via the Sig1R (Yamamoto et al., 1995; Bergeron et al., 1996; Karasawa et al., 2002; Zhang et al., 2011). Note, however, that the Sig1R may not necessarily be interacting directly with the NMDAR; for example, (+)pentazocine potentiates NMDAR-mediated responses via the Sig1R-mediated inhibition of Ca^{2+}-activated K^+ channels [SK channels (Martina et al., 2007)]. It has also been proposed that the Sig1R ligands SKF-10047 and haloperidol can antagonize the NMDAR directly, rather than through the Sig1R (Kume et al., 2002).

There have been conflicting results regarding the subunit arrangement in the GluN1/GluN2A NMDAR, with evidence for either an adjacent (Schorge and Colquhoun, 2003) or an alternating (Salussolia et al., 2011) arrangement. Recently, we used AFM imaging of receptors decorated by subunit-specific antibodies to show that the GluN1/GluN2A NMDAR adopts an adjacent (i.e., 1/1/2/2) subunit arrangement (Balasuriya et al., 2013). In the present study, we show that pairs of Sig1Rs decorate the NMDAR at a mean angle of 72°, a result that again indicates an adjacent arrangement of the two GluN1 subunits. Interestingly, decoration of the GluN1 dimers by pairs of Sig1Rs occurred at a very similar angle (80°), suggesting that pairs of GluN1 subunits assemble to form homodimers with an arrangement similar to that seen within the assembled GluN1/GluN2A NMDAR, an event that might normally represent the first step in NMDAR assembly, as suggested previously (Meddows et al., 2001; Papadakis et al., 2004; Farina et al., 2011).

The *in situ* proximity ligation assays demonstrate that the interaction between the Sig1R and GluN1 (but not GluN2A) occurs within cells as well as *in vitro*. The proximity signal, like the immunofluorescence signals for the various proteins, is distributed throughout the cell cytoplasm, indicating that the interaction between the Sig1R and the NMDAR is not restricted to the plasma membrane. Consistent with this widespread intracellular location, Sig1R has been shown previously to perform a chaperoning function, increasing the delivery of channels such as hERG (Crottès et al., 2011) to the plasma membrane; such an effect may also occur with the NMDAR. On the other hand, there is also evidence that ion channel function, including that of the NMDAR (Zhang et al., 2011), can be rapidly modulated via the Sig1R, indicating an interaction at the plasma membrane.

The arrangement of the Sig1R in the membrane has been controversial, with evidence, based on immunofluorescence using antibodies against known sites, that the N and C termini are either cytoplasmic (Aydar et al., 2002) or extracytoplasmic (Hayashi and Su, 2007; Kourrich et al., 2013). Using *in situ* proximity ligation, we show here that that the C terminus (and, consequently, the N terminus also) is extracytoplasmic.

In conclusion, we show that the Sig1R binds directly to the GluN1/GluN2A NMDAR specifically via GluN1 and that this interaction occurs both *in vitro* and within cells. This interaction likely accounts for some of the known effects of Sig1R ligands on NMDAR function and may be relevant to the important roles played by the Sig1R in the CNS.

References

Aydar E, Palmer CP, Klyachko VA, Jackson MB (2002) The sigma receptor as a ligand-regulated auxiliary potassium channel subunit. Neuron 34: 399–410. CrossRef Medline

Balasuriya D, Stewart AP, Crottès D, Borgese F, Soriani O, Edwardson JM (2012) The sigma-1 receptor binds to the Nav1.5 voltage-gated Na^+ channel with 4-fold symmetry. J Biol Chem 287:37021–37029. CrossRef Medline

Balasuriya D, Goetze TA, Barrera NP, Stewart AP, Suzuki Y, Edwardson JM (2013) AMPA and NMDA receptors adopt different subunit arrangements. J Biol Chem 288:21987–21998. CrossRef Medline

Bergeron R, de Montigny C, Debonnel G (1996) Potentiation of neuronal NMDA response induced by dehydroepiandrosterone and its suppression by progesterone: effects mediated via sigma receptors. J Neurosci 16: 1193–1202. Medline

Carnally SM, Johannessen M, Henderson RM, Jackson MB, Edwardson JM (2010) Demonstration of a direct interaction between sigma-1 receptors and acid-sensing ion channels. Biophys J 98:1182–1191. CrossRef Medline

Crottès D, Martial S, Rapetti-Mauss R, Pisani DF, Loriol C, Pellissier B, Martin P, Chevet E, Borgese F, Soriani O (2011) Sig1R protein regulates hERG channel expression through a post-translational mechanism in leukemic cells. J Biol Chem 286:27947–27958. CrossRef Medline

Farina AN, Blain KY, Maruo T, Kwiatkowski W, Choe S, Nakagawa T (2011) Separation of domain contacts is required for heterotetrameric assembly of functional NMDA receptors. J Neurosci 31:3565–3579. CrossRef Medline

Hayashi T, Su TP (2007) Sigma-1 receptor chaperones at the ER-mitochondrion interface regulate Ca^{2+} signaling and cell survival. Cell 131:596–610. CrossRef Medline

Hayashi T, Kagaya A, Takebayashi M, Shimizu M, Uchitomi Y, Motohashi N, Yamawaki S (1995) Modulation by sigma ligands of intracellular free Ca^{++} mobilization by N-methyl-D-aspartate in primary culture of rat frontal cortical neurons. J Pharmacol Exp Ther 275:207–214. Medline

Ishiguro H, Ohtsuki T, Toru M, Itokawa M, Aoki J, Shibuya H, Kurumaji A, Okubo Y, Iwawaki A, Ota K, Shimizu H, Hamaguchi H, Arinami T (1998) Association between polymorphisms in the type 1 sigma receptor gene and schizophrenia. Neurosci Lett 257:45–48. CrossRef Medline

Karasawa J, Yamamoto H, Yamamoto T, Sagi N, Horikomi K, Sora I (2002) MS-377, a selective sigma receptor ligand, indirectly blocks the action of PCP in the N-methyl-D-aspartate receptor ion-channel complex in primary cultured rat neuronal cells. Life Sci 70:1631–1642. CrossRef Medline

Kourrich S, Hayashi T, Chuang JY, Tsai SY, Su TP, Bonci A (2013) Dynamic interaction between sigma-1 receptor and Kv1.2 shapes neuronal and behavioral responses to cocaine. Cell 152:236–247. CrossRef Medline

Kume T, Nishikawa H, Taguchi R, Hashino A, Katsuki H, Kaneko S, Minami M, Satoh M, Akaike A (2002) Antagonism of NMDA receptors by sigma receptor ligands attenuates chemical ischemia-induced neuronal death in vitro. Eur J Pharmacol 455:91–100. CrossRef Medline

Lysko PG, Feuerstein G (1990) Excitatory amino acid neurotoxicity at the N-methyl-D-aspartate receptor in cultured neurons: protection by SKF 10,047. Neurosci Lett 120:217–220. CrossRef Medline

Lysko PG, Gagnon RC, Yue TL, Gu JL, Feuerstein G (1992) Neuroprotective effects of SKF 10,047 in cultured rat cerebellar neurons and in gerbil global brain ischemia. Stroke 23:414–419. CrossRef Medline

Martina M, Turcotte ME, Halman S, Bergeron R (2007) The sigma-1 receptor modulates NMDA receptor synaptic transmission and plasticity via SK channels in rat hippocampus. J Physiol 578:143–157. CrossRef Medline

Maurice T, Su TP (2009) The pharmacology of sigma-1 receptors. Pharmacol Ther 124:195–206. CrossRef Medline

Meddows E, Le Bourdellès B, Grimwood S, Wafford K, Sandhu S, Whiting P, McIlhinney RA (2001) Identification of molecular determinants that are important in the assembly of N-methyl-D-aspartate receptors. J Biol Chem 276:18795–18803. CrossRef Medline

Papadakis M, Hawkins LM, Stephenson FA (2004) Appropriate NR1-NR1 disulfide-linked homodimer formation is requisite for efficient expression of functional, cell surface N-methyl-D-aspartate NR1/NR2 receptors. J Biol Chem 279:14703–14712. CrossRef Medline

Salussolia CL, Prodromou ML, Borker P, Wollmuth LP (2011) Arrangement of subunits in functional NMDA receptors. J Neurosci 31:11295–11304. CrossRef Medline

Schneider SW, Lärmer J, Henderson RM, Oberleithner H (1998) Molecular weights of individual proteins correlate with molecular volumes measured by atomic force microscopy. Pflügers Arch 435:362–367. CrossRef Medline

Schorge S, Colquhoun D (2003) Studies of NMDA receptor function and stoichiometry with truncated and tandem subunits. J Neurosci 23:1151–1158. Medline

Scott DW (1979) On optimal and data-based histograms. Biometrika 66:605–610. CrossRef

Söderberg O, Gullberg M, Jarvius M, RidderstråleK, Leuchowius KJ, Jarvius J Wester K, Hydbring P, Bahram F, Larsson LG, Landegren U (2006) Direct observation of individual endogenous protein complexes in situ by proximity ligation. Nat Methods 3:995–1000. CrossRef Medline

Su TP, Hayashi T, Maurice T, Buch S, Ruoho AE (2010) The sigma-1 receptor chaperone as an inter-organelle signaling modulator. Trends Pharmacol Sci 31:557–566. CrossRef Medline

Tchedre KT, Huang RQ, Dibas A, Krishnamoorthy RR, Dillon GH, Yorio T (2008) Sigma-1 receptor regulation of voltage-gated calcium channels involves a direct interaction. Invest Ophthalmol Vis Sci 49:4993–5002. CrossRef Medline

Traynelis SF, Wollmuth LP, McBain CJ, Menniti FS, Vance KM, Ogden KK, Hansen KB, Yuan H, Myers SJ, Dingledine R (2010) Glutamate receptor ion channels: structure, regulation, and function. Pharmacol Rev 62:405–496. CrossRef Medline

Waxman EA, Lynch DR (2005) N-methyl-D-aspartate receptor subtypes: multiple roles in excitotoxicity and neurological disease. Neuroscientist 11:37–49. CrossRef Medline

Welch BL (1947) The generalisation of student's problems when several different population variances are involved. Biometrika 34:28–35. CrossRef Medline

Yamamoto H, Yamamoto T, Sagi N, Klenerová V, Goji K, Kawai N, Baba A, Takamori E, Moroji T (1995) Sigma ligands indirectly modulate the NMDA receptor-ion channel complex on intact neuronal cells via sigma 1 site. J Neurosci 15:731–736. Medline

Zhang XJ, Liu LL, Jiang SX, Zhong YM, Yang XL (2011) Activation of the sigma receptor 1 suppresses NMDA responses in rat retinal ganglion cells. Neuroscience 177:12–22. CrossRef Medline